UKACC International Conference on Control 2012
Cardiff, UK, 3-5 September 2012

Adaptive Feed-Forward and Feedback Control for Oxygen Ratio in Fuel Cell Stacks

Omar Ragb, D L YU and JB Gomm
Control system research group, School of Engineering
Liverpool John Moore University
Liverpool, UK
om.khazali_yo@yahoo.com

Abstract—**Automatic control of fuel cell stacks (FCS) using non-adaptive and adaptive radial basis function (RBF) neural network methods are investigated in this paper. The neural network RBF inverse model is used to estimate the compressor voltage for fuel cell stack control at different current demands, reduction in the compressor gain (30% and 20%) and manifold leak (15%) in order to prevent the oxygen starvation. A PID controller is used in the feedback to adjust the difference between the requested and the actual oxygen ratio by compensating the neural network inverse model output. This method is designed and conducted in three stages, starting with the collection of data from the available fuel cell stack model and finished with the non adaptive and adaptive RBF neural network control. RBF neural networks with the K-means and P-nearest Neighbour's training algorithms are used for the investigation. Furthermore, the RBF inverse model is made adaptive to cope with the significant parameter uncertainty, disturbances and environment changes. Simulation results show the effectiveness of the adaptive control strategy.**

Keywords-Fuel cell stacks; Non-adaptive; Adaptive; Radial Basis Function Neural Network; Feed-forward; Feedback oxygen starvation.

I. INTRODUCTION

Burning current natural sources causes many environment problems today. A lot of harmful gases, such as CO_2, rise in the environment as a result of burning fossil fuels and destructs the ozone layer, which leads to climatic change and what is known as the greenhouse effect. To recover this problem, the world has been looking for energy sources that are clean and safe on the environment. Fuel cells are a kind of clean and safe energy source on the environment. Polymer electrolyte membrane (PEM) fuel cells emerge as one of the most clean and promising alternatives to reduce fossil fuel dependency [1]. In the last years many researchers have presented some methods to control the fuel cell stacks, in order to prevent the oxygen starvation and improve the fuel cell control, which are now reviewed. Sedighizadeh M. [2] discussed the application of wavelet networks in the implementation of adaptive controllers for PEMFC's. Jiang Z. et al. [3] presented an adaptive control strategy for active power sharing in the hybrid power source. This control strategy is able to adjust the output current set-point of the fuel cell according to the state of the charge (or voltage) of the battery. An adaptive MPPT controller using the extrermum-seeking algorithm [4] is used to automatically keep the fuel cell working at maximum power point (MPP) all the time. Fiacchini M. et al. [5] is presented an adaptive control scheme for the safe operation of a fuel cell system. In particular, the aim of control action is to avoid that the oxygen ratio reaches dangerous values. In this paper adaptive and non-adaptive control methods are implemented to achieve better control for the fuel cell breathing. Furthermore, in this paper, we first explain the fuel cell working principles followed by description of the dynamic model of fuel cell stacks. We then formulate the RBF adaptive and non adaptive model. Finally we demonstrate simulation results for the fuel cell control with adaptive and non adaptive controllers.

II. FUEL CELL DYNAMICS

A. Fuel Cell Working and prenceples

Fuel cells consume a hydrogen fuel (on the anode side) and oxygen (on the cathode side) and produce electric energy with water and some heat through a chemical reaction [1], to satisfy different power requirements (Fig. 1). Generally, the reactants flow in and reaction products flow out while the electrolyte remains in the cell. Fuel cells differ from batteries in that they do not need recharging, they operate quietly and efficiently, and when hydrogen is used as fuel they generate only electric power and drinking water. So, they are called zero emission engines. William Grove discovered the basic operating principle of fuel cells by reversing water in 1839 [6]. In particular, proton exchange membrane fuel cells (PEM-FCs), also known as polymer electrolyte membrane fuel cells, are considered to be more developed than other fuel cells technologies, because they have high power density, solid electrolyte, operate at low temperature, long cell and stack life and low corrosion [6]. The PEM-FC takes its name from the special plastic membrane used as the electrolyte. This membrane electrode assembly (MEA), not thicker than a few hundred microns, is the heart of a PEM-FC and, when supplied with fuel and air, generates electric power at cell voltages around 0.7 Volt and power densities of up to about 1 W/cm electrode area. Fig. 2 shows a schematic of a PEM-FCS and MEA. The MEA is typically located between a pair of current collector plates (platinum-impregnated porous electrodes) with machined flow fields for distributing fuel and oxidant to the

Omar AL-Mukhtar University, Libya

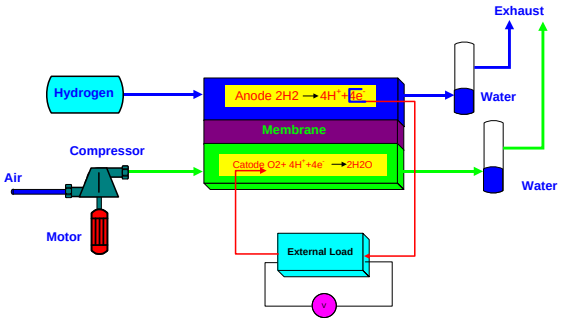

Figure 1. PME- FC reaction and structure

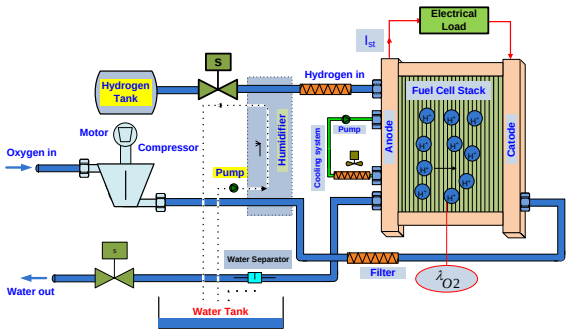

Figure 2. PEM fuel cell structure

anode and cathode, respectively. A water jacket for cooling is often placed at the back of each reactant flow field followed by a metallic current collector plate. The cell can also contain a humidification section for the reactant gases, which are kept close to their saturation level in order to prevent dehydration of the membrane electrolyte. Many FCs are connected electrically in series (Fig. 2) to form an FC stack (FCS).

B. *Fuel Cell Stack Model*

The fuel cell stack (FCS) model simulated in this paper consists of four interacting sub-models (Fig. 3) which are the stack voltage, the anode flow, the cathode flow, and the membrane hydration models [6]. The voltage model contains an equation to calculate stack voltage based on fuel cell temperature, pressure, reactant gas partial pressures and membrane humidity, in summary, the fuel cell voltage E is given by

$$E = 1.2229 - 0.85\times10^{-3}(T_{fc} - 29815) + 43085\times10^{-5}T_{fc}(p_{H2}) + \frac{1}{2}p_{O2} \quad (1)$$

where, T_{fc} is the fuel cell temperature in Kelvin, p_{H2} and p_{O2} are the partial pressures of hydrogen and oxygen respectively, details in [1,6]. In this model the stack temperature is assumed to be constant at 80°C. The model which is used in our investigations is given in [6]. The FCS Simulink model is created in Matlab 6.5.

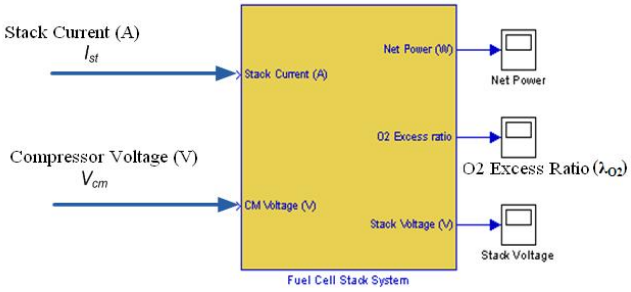

Figure 3. Simulink model of integrated PEM fuel cell

III. FEED-FORWARD CONTROL DESIGN BASED ON NN

A. *NN Inverse Model*

The radial basis function neural network (RBFNN) has an ability to model any non-linear function. However, this kind of neural network can need many nodes to achieve the required approximating properties [7]. The first step in the fuel cell modelling is the generation of a suitable training data set. The accuracy of the neural network modelling performance will be influenced by the training data. In the fuel cell stack data collection, the training data must be representative fuel cell behavior in order to analyze the performance of RBF fuel cell models in practical operating conditions. This means that input and output signals should sufficiently cover the region in which the system is going to be controlled [8]. As shown in Fig. 3, the fuel cell stack used for this research has to inputs compressor voltage v_{cm} and the load current I_{st}, has three outputs (stack voltage SV, net power NP and oxygen ratio $y=O_2$). A set of random amplitude signals (RAS) were designed (0~3000 samples) for the fuel cell current load demand (I_{st}) and the compressor voltage (v_{cm}) to obtain a representative set of input data. The RASs of the current load demand and fuel cell compressor voltage were bounded between 100 and 300 Ampere for the current and between 100 and 235 volts for the compressor voltage see table I. Appling these two random input signals on the fuel cell model produces three outputs which are oxygen ratio (y), stack voltage (SV) and net power (NP) see table II and Fig. 4.

TABLE I. RAS INPUTS SIGNAL FOR $\hat{v}_{cm}$ MODELLING

Parameters	Minimum	Maximum
v_{cm}	100 Volts	235 Volts
I_{st}	100	300

TABLE II. OUTPUTS SIGNAL FOR $\hat{v}_{cm}$ MODELLING

Parameters	Minimum	Maximum
$y=O_2$	0.7051	5.24
SV	112.64 Volts	282.79 Volts
PN	3850	6630

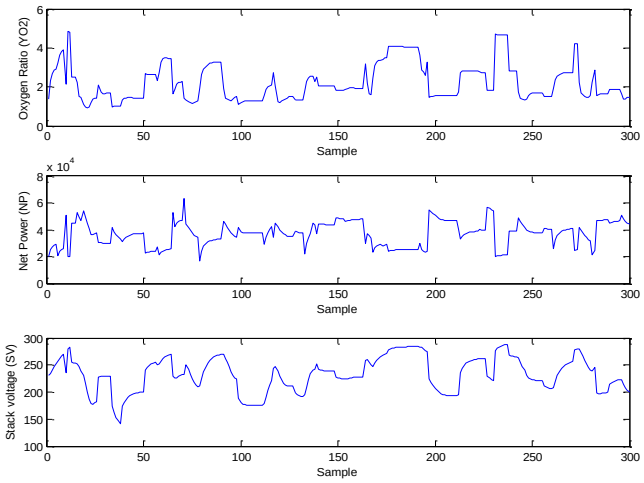

Figure 4. Fuel cell stack parameters output after applied RAS of I_{st} & v_{cm}

For RBF neural network training, the K-means algorithm is used to choose the centers, ρ-nearast neighbor algorithm decides the widths and the recursive training algorithm [9] calculates the weights for the output layer. Here, a RBFNN based inverse model is used to predict the compressor voltage $\hat{v}_{cm}(k)$ which is the manipulated variable in the next sample time.The RBFNN block diagram is illustrated in Fig. 5, where the RBFNN input at sample k is a vector $x(k)$ it also given by the following equation:

$$x(k) = [v_{cm}(k-1)\ y(k-1)\ I_{st}(k)\ I_{st}(k-1)\ SV(k-1)\ PN(k-1)\ PN(k-2)\ PN(k-3)]^T \quad (2)$$

The neural network output is:

$$\hat{v}_{cm}(k) = g[v_{cm}(k-1)\ y(k-1)\ I_{st}(k)\ I_{st}(k-1)\ SV(k-1)\ N(k-1)\ PN(k-2)\ PN(k-3)] \quad (3)$$

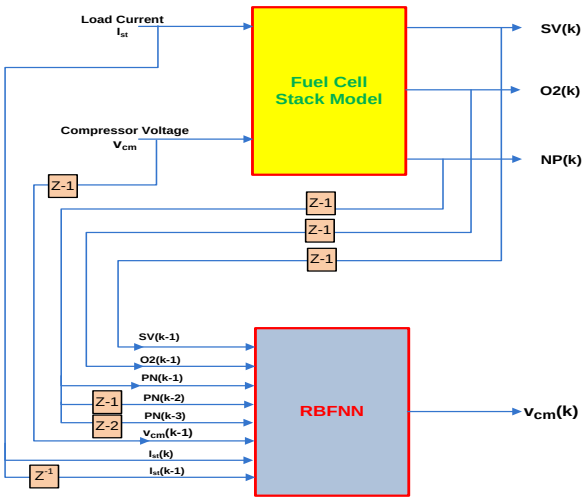

Figure 5. The RBFNN block diagram with Input variables

where g(.) is the nonlinear neural network function and $\hat{v}_{cm}(k)$ is the estimated compressor voltage. In order to train this neural network model, RASs were applied to the two fuel cell stack inputs I_{st} and v_{cm} and data for the fuel cell were collected for O_2, SV and PN at each sample time. The raw data were scaled using the following equation before training:

$$xscale(k) = \frac{x(k) - \min\{x(i)\}}{\max\{x(i)\} - \min\{x(i)\}} \qquad i \in [1, N]$$

The training data set with 2000 samples are used to train the RBFNN model. Then, the test set with 1000 is applied to the trained model and the model output prediction results are displayed in Fig. 6. The mean absolute error (MAE) is used to evaluate the modelling and control performance in this research, which is given by the following equation:

$$MAE = \frac{1}{N}\sum_{k=1}^{N}\left|\hat{v}_{cm}(k) - v_{cm}(k)\right| = \frac{1}{N}\sum_{k=1}^{N}\left|e(k)\right| \quad (5)$$

where $\hat{v}_{cm}(k)$ is the prediction by the inverse neural network model and v_{cm} is the compressor voltage. The $\hat{v}_{cm}(k)$ in Fig. 6 is the normalized value and the MAE is 0.0142. The output of the neural network is nearly equal to the actual compressor voltage input. This is because *y(k-1)*, which can be calculated online at sample time *k*, was also used to predict the value of compressor voltage $\hat{v}_{cm}(k)$. Also this inverse RBFNN model can predict the required $\hat{v}_{cm}(k)$ for one sample step. The $\hat{v}_{cm}(k)$ can be calculated according to (3).

B. Non-Adaptive FF and FB Control Scheme

The RBFNN-based non-adaptive feed-forward with feedback control system structure in our implementation is shown in Fig. 7. After trained the RBFNN inverse model and we got satisfy results. So, all the Recursive Least Square parameters (*w(0)*,μ and *ρ(0)* will be saved in order to use them in non-adaptive and adaptive feed-forward controllers, then we will use this model in the feed-forward path to predict the scaled compressor voltage $\hat{v}_{cm}(k)$ and is given by (6).

$$\hat{v}_{cm}(k) = \phi^T \times w \quad (6)$$

So, to get the non scaled compressor voltage the (7) should be applied:

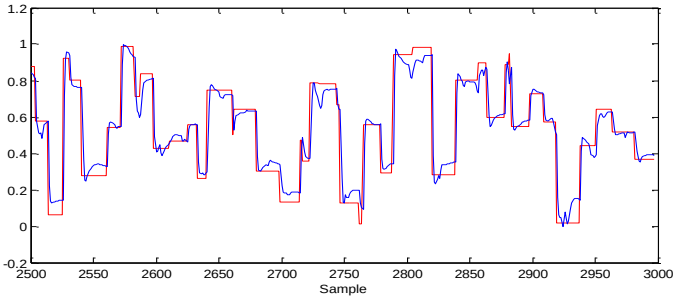

Figure 6. v_{cm} Validation data for RBFNN model MAE (Mean Absolute Errors=0.0142)

$$v_{cm}(k) = \min v_{cm} + \hat{v}_{cm}(k) + \max v_{cm} - \min v_{cm}) \quad (7)$$

On the other hand, to enhance the performance in steady state, the PID controller is added to form the feedback controller. In this case the activating compressor voltage is the sum of two controller outputs variables, one is from the RBF based feed-forward neural network controller, the other from the feedback PID controller. The current demand changing during the control is shown in Fig. 8. The following digital PID controller equation is used in [9]:

$$v_{cm\,2}(k) = y(k-1) + K_p\left[\left(1+\frac{T}{T_i}+\frac{T_d}{T}\right)e(k) - \left(1+\frac{2T_d}{T}\right)e(k-1) + \frac{Td}{T}e(k-2)\right] \quad (8)$$

After fine tuning, the PID controller that is used here with RBF based neural network controller for oxygen ratio regulation is

$$\hat{v}_{cm2}(k) = y(k-1) + 585e(k) - 45e(k-1)2.2\times10^{-4}e(k-2) \quad (9)$$

Here the sampling time is chosen to be 0.1sec. The measured oxygen ratio with time delay is the feedback signal of system.

C. *Adaptive FF and FB Control Scheme*

The different of the strategy of adaptive RBFNN based FF control of oxygen ratio is the widths and the weights will be updated at each sample time. The RBF-NN based adaptive feed-forward and feedback control system structure is illustrated in Fig. 9. After training the RBFNN inverse model and we got satisfy good match. The PID controller is added to form the feedback control as discussed in the non-adaptive control.

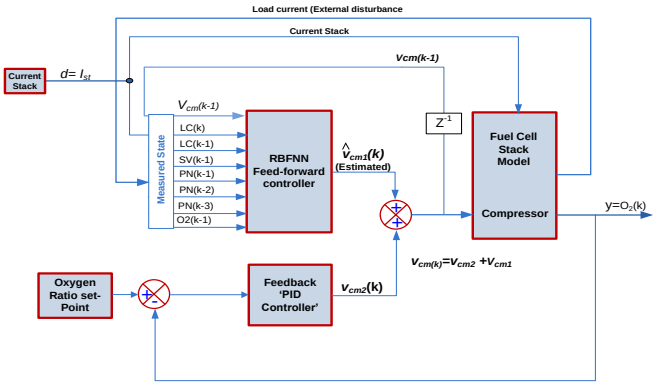

Figure 7. RBFNN FF and PID controller on the FCs

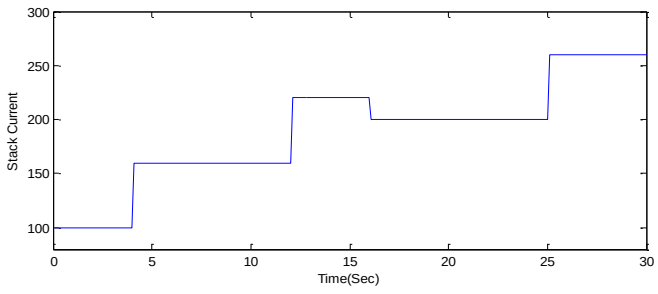

Figure 8. Fuel cell current demand changing during the control

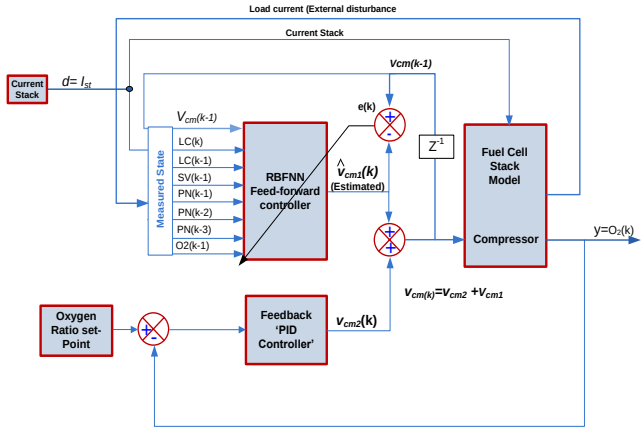

Figure 9. RBFNN FF and PID Controller on the Fuel Cell Stack

IV. SIMULATION RESULTS

The output responses simulation of the oxygen ratio for non-adaptive and adaptive RBFNN feed-forward control for fuel cell stack are illustrated in fig. 10 and 11, the significant a difference can be seen between the performances of the two controllers. The tracking MAE of oxygen for non-adaptive and adaptive are 0.0045 and 0.0036 respectively.

A. *Control Performance with 30% and 20% Reduction in the Compressor Gain*

The compressor is a machine to press the air inside the cathode but in some cases there are some problems associated with the compressor, which leads to reduce efficiency of the compressor.

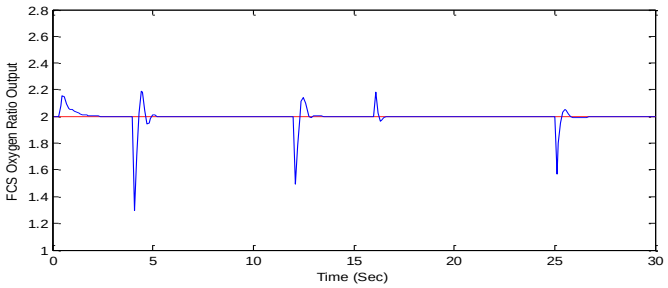

Figure 10. Simulation Result of Non-Adaptive RBF-Based FF & FB Control on FCS Oxygen Ratio

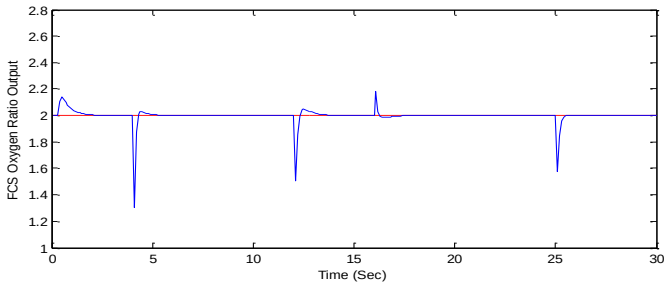

Figure 11. Simulation Result of Adaptive RBF-Based FF & FB Control on FCS Oxygen Ratio

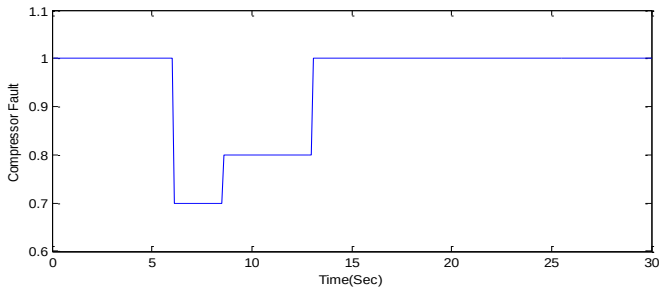

Figure 12. FCS Compressor Efficiency Fault Simulation

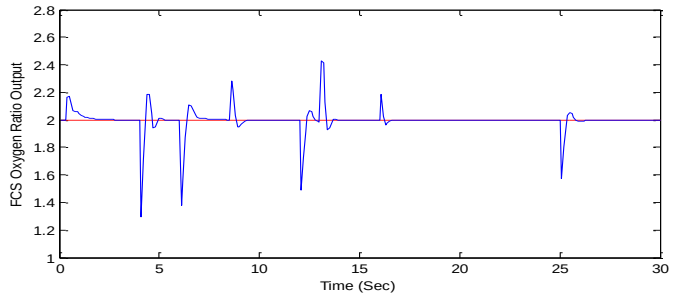

Figure 13. Simulation Result of Non-Adaptive FF and FB Controller on O_2 with 30~ 20% Reduction in Compressor Gain

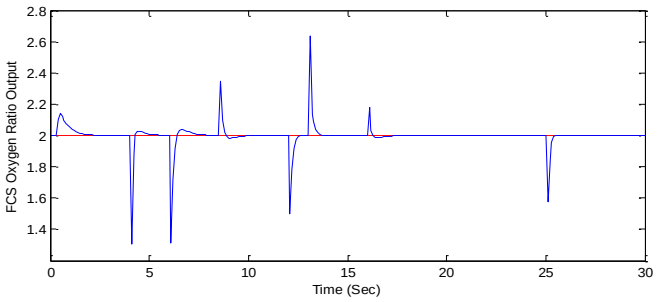

Figure 14. Simulation of Adaptive FF and FB Control on O_2 Ration With 30~20% Reduction In Compressor Gain

So, it needs regular maintenance because it contains gears and movement parts with oil circulation. When there is a problem in any part will affect on the efficiency of the compressor. The adaptive and non-adaptive RBFNN feed-forward controllers are evaluated with the current signal demand (Fig. 8) and the compressor gain reduction (Fig. 12). After reducing the compressor gain by 30% and 20% respectively, which will decrease the value of O_2 flow into the FCS port, the non-adaptive RBFNN model has a little capability to deal with this problem because it cannot retune itself according to this error, as a result it can't overcome this change and its MAE is 0.0083 (Fig. 13). However the adaptive RBF has the capability to retune itself to cope this situation and hence, achieves an improved control performance with a mean absolute error of 0.0075 (Fig. 14).

B. Control Performance with Compressor Gain Reduction and Manifold Leak

Manifold leak is called component fault and to represent the air leakage fault, the manifold pressure equation in [6] is modified to (10):

$$\frac{dm_{sm}}{dt} = W_{cp} - W_{sm} - \Delta L \tag{10}$$

Where, W_{cp} is the inlet mass flow (compressor flow), W_{sm} is the supply manifold outlet mass flow and the added term ΔL is used to simulate the leakage from the supply air manifold, which decrease the air outflow from the manifold. $\Delta L = 0$ represents no air leak in the intake manifold. The air leakage level is simulated as 15% of total air intake in manifold as shown in Fig.15, and was simulated by changing the Simulink model of the FCS. From the oxygen ratio output shown in Fig. 16, the performance of non adaptive RBF FFC is acceptable and the MAE is 0.0126%. However, the performance of the adaptive RBF FFC as shown in Fig. 17 is better than the non adaptive. The adaptive RBF FFC can handle the manifold leak and therefore, achieves an improved control performance with mean MAE equal to 0.0090.

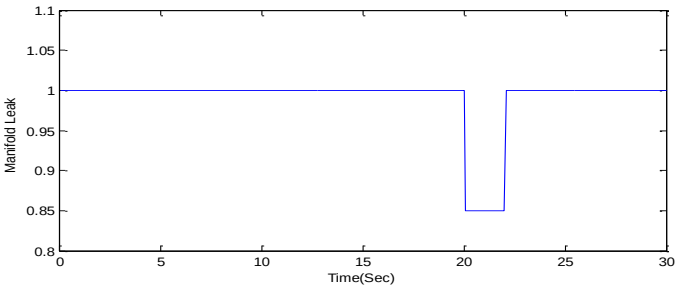

Figure 15. Manifold leak error simulate

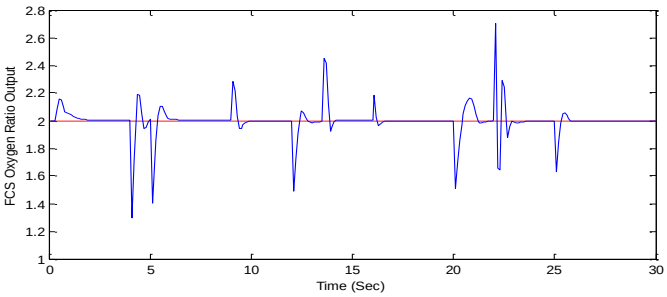

Figure 16. Oxygen ratio control result of the non adaptive RBF FFC with compressor gain reduction and leak

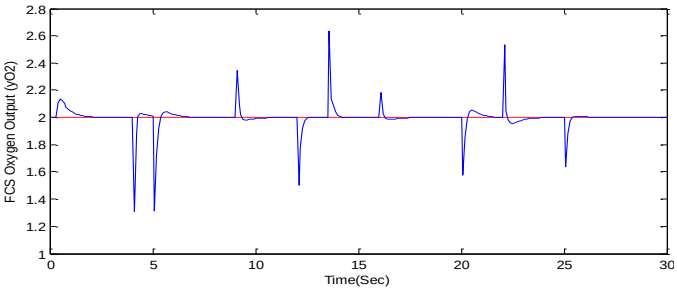

Figure 17. Oxygen ratio control result of the adaptive RBF FFC with compressor gain reduction and leak

TABLE III. EVALUATED

Type of control method	Mean Absolute Error MAE
Non-adaptive RBFNN Control+PID controller	0.0045
Adaptive RBFNN +PID controller	0.0036
Non-adaptive RBFNN Control+PID controller with compressor gain reduction 30% and 20%	0.0087
Adaptive RBFNN Control+PID controller with compressor gain reduction 30% and 20%	0.0075
Non adaptive RBFNN Control+PID controller with compressor gain reduction 30% and 20% and the manifold leak 15%	0.0126
Adaptive RBFNN Control+PID controller with compressor gain reduction 30% and 20% and the manifold leak 15%	0.0090

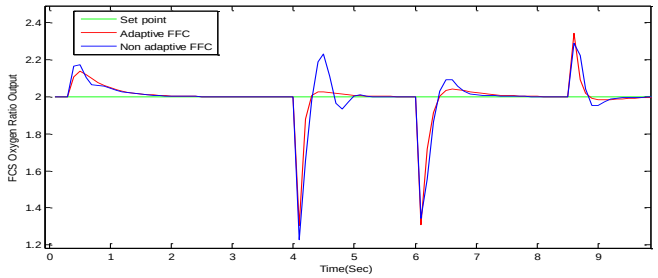

Figure 18. Comparing Adaptive and Non-Adaptive Control Performance when there is gain reduction

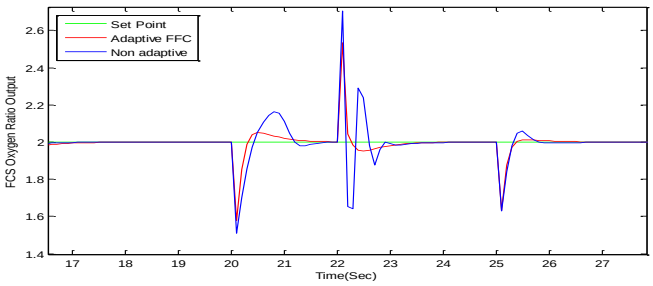

Figure 19. Comparing Adaptive and Non-Adaptive Control Performance when there are gain reduction and manifold leak

V. DISCUSSION

From the Fig. 10 and 11 and the table III, when there is no reduction in the compressor gain, the RBFNN adaptive can give good performance than non-adaptive FFC with MAE equal to 0.0036 and 0.0045 respectively. However, reducing the compressor gain by 30% and 20% respectively, which will decrease the value of O_2 flow into the FCS port, the non-adaptive RBF controller has little capacity to deal with this situation because it was trained off-line and is fixed. As result it was unable to cope with an environment change see Fig. 13. However, the adaptive RBFNN can adjust the compressor voltage according to the real-time condition of the FCS and compensate for the influence of this system error after several sample times see Fig. 14. Fig. 18 show the comparison on oxygen ratio rates between Fig. 13 and 14. After that, the performance of the non adaptive and adaptive RBF FFC is evaluated with manifold leak Fig. 15 additional to current disturbance Fig. 8 and compressor gain reduction Fig. 12, the simulation results are as given in Fig. 16 and 17. The adaptive performance also, has more capacity to overcome the environmental change than the non adaptive because it was trained on-line according to the error see table III and Fig. 19.

VI. CONCLUSION AND FUTURE WORK

This paper presents an adaptive and non-adaptive RBF control strategy to estimate the compressor voltage for fuel cell stack control to prevent fuel cell oxygen starvation and compressor surge during rapid load demands, gain reduction (30% and 20%) and manifold leak 15%. APID controller is used in the feedback to adjust the difference between the requested and the actual oxygen ratio by compensating the neural network inverse model output. When there is no reduction in the compressor gain the control strategy can adjust the compressor voltage of the fuel cell according to the current demand. From the other hand, when there is reduction (30% and 20%) in the compressor gain and 15% manifold leak. The non-adaptive RBF controller less ability than adaptive RBF controller because the adaptive was trained off-line, as a result it was unable to cope with an environmental changes. Furthermore, the adaptive RBFNN is able to adjust the compressor voltage to adapt to the real-time condition of the FCS and compensate for the influence of this system error after several sample times. The simulation results show the effectiveness of the adaptive control strategy.

REFERENCES

[1] J. T. Pukrushpan, A. G. Stefanopoulou, and H. Peng, "Control of fuel cell breathing," IEEE ControlSystems Magazine, vol. 24, no. 2, pp. 30-46, April 2004.

[2] M. Sedighizadeh, and A. Rezazadeh, "A Neuro adaptive control Strategy for movable power source of proton exchange membrane fuel cell using wavelets," World Academy of Science, Engineering and Technology, vol. 36, pp. 285 -289, 2007.

[3] Z. Jiang, L. Gao, and A. Roger, "Adaptive control strategy for active power sharing in hybrid fuel cell/battery power sources," IEEE Transactions on Energy Conversion, vol. 22, No. 2, pp. 507-515, 2007.

[4] Z. Zhong, H. Hai-bo, X. Zhu, C. Guang-yi and R. Yuan, "Adaptive maximum power point tracking control of fuel cell power plants," Elsever Journal of Power Sources, vol. 176, pp. 259-269, 2008.

[5] M. Fiacchini, T. Alamo, C. Albea, and F. Camacho, "Adaptive model predictive control of the hybrid dynamics of a fuel cell system, control application," IEEE International Conference on, Singapore. DOI: 10.1109/CCA., 2007. 4389435.

[6] J. T. Pukrushpan, A. G. Stefanopoulou, and H. Peng, "Control of fuel cell power systems, springer," vol. 13, No. 1, pp. 3-14, 2004.

[7] Y. J. Zhai, and D. L. Yu, "Radial-basis-function-based feedforward–feedback control for air–fuel ratio of spark ignition engines," School of Engineering, LJMU, Liverpool, UK, vol. 222 Part D: J. Automobile Engineering, pp. 416-428, 2007.

[8] Y.J. Zhai, D.L.Yu, Reza T., Y. Al-Hamidi, "Fast predictive control for air-fuel ratio of SI engines using a nonlinear internal model," international Journal of Engineering, Science and Technology, vol. 3, No. 6, 2011, pp. 1-17, 2011.

[9] Kristine Z. T., L. Bell, and L. Harry, T. Van, "A recursive least squares implementation for lcmp beamforming under quadratic constraint," IEEE Transactions on Signal Processing, vol. 49. No. 6, 2001.